Phytopathology® • 2025 • 115:374-386 • https://doi.org/10.1094/PHYTO-03-24-0107-R

Fungal Biology and Genetics

A Family of Transglutaminases Is Essential for the Development of Appressorium-Like Structures and *Phytophthora infestans* Virulence in Potato

Maja Brus-Szkalej,[1,†] Bradley Dotson,[1] Christian B. Andersen,[1] Ramesh R. Vetukuri,[2] and Laura J. Grenville-Briggs[1]

[1] Department of Plant Protection Biology, Swedish University of Agricultural Sciences, Box 190, 234 22 Lomma, Sweden
[2] Department of Plant Breeding, Swedish University of Agricultural Sciences, Box 190, 234 22 Lomma, Sweden
Accepted for publication 20 December 2024.

Abstract

Transglutaminases (TGases) are enzymes highly conserved among prokaryotic and eukaryotic organisms, where their role is to catalyze protein cross-linking. One of the putative TGases of *Phytophthora infestans* has previously been shown to be localized to the cell wall. Based on sequence similarity, we were able to identify six more genes annotated as putative TGases and show that these seven genes group together in phylogenetic analysis. These seven proteins are predicted to contain both a TGase domain and a MANSC domain, the latter of which was previously shown to play a role in protein stability. Chemical inhibition of TGase activity and silencing of the entire family of the putative cell wall TGases are both lethal to *P. infestans*, indicating the importance of these proteins in cell wall formation and stability. The intermediate phenotype obtained with lower drug concentrations and less efficient silencing displays a number of deformations to germ tubes and appressoria. Both chemically treated and silenced lines show lower pathogenicity than the wild type in leaf infection assays. Finally, we show that appressoria of *P. infestans* possess the ability to build up turgor pressure and that this ability is decreased by chemical inhibition of TGases.

Keywords: cell wall, chemical inhibition, oomycete biology, potato late blight, RNAi, silencing, transglutaminase, turgor pressure

Transglutaminases (TGases) are a group of enzymes (EC 2.3.2.13) that catalyze acyl transfer reactions between γ-carboxamide groups of peptide-bound glutamine and a wide variety of acceptor substrates, usually amino acids (Folk 1980). Of most interest, and hence the best studied reaction catalyzed by TGases, is the interaction with ε-amino groups of peptide-bound lysine residues resulting in inter- or intramolecular protein cross-linking (ε-(γ-glutamyl)lysine cross-link) (Folk 1980; Lorand and Graham 2003). Although first discovered and extracted from animal tissue (Folk and Cole 1966; Sarkar et al. 1957), TGases are widely conserved among both prokaryotic and eukaryotic organisms (Griffin et al. 2002; Martins et al. 2014; Parrotta et al. 2022). The conservation of enzymatic properties in different organisms has therefore allowed for replacement of the previously used guinea pig TGase by the cheaper and ethically preferable microbial transglutaminase in food manufacturing (Kieliszek and Misiewicz 2014; Martins et al. 2014). The biological roles of TGases are still best characterized for humans, where all nine TGases have been assigned to different organs, and a specific function has been assigned to eight of them (Eckert et al. 2014).

†Corresponding author: M. Brus-Szkalej; maja.brus@slu.se

Funding: Support was provided by the European Union's Horizon 2020 Research and Innovation Program (grant 766048; MSCA-ITN-2017 PROTECTA), the Swedish Research Council FORMAS (grant 2019-00881 to L. J. Grenville-Briggs), and the Swedish Research Council Vetenskapsrådet (grant 2023-05529 to L. J. Grenville-Briggs).

***e*-Xtra:** Supplementary material is available online.

The author(s) declare no conflict of interest.

Interestingly, although plant TGases do not show high sequence similarity to those from animals, they do resemble them structurally and can interact with animal TGase antibodies (Beninati et al. 2013). The main functions of plant TGases are usually linked to photosynthesis, responses to stress, senescence, and programmed cell death, and it is believed they do so through stabilization and modification of various proteins involved in these processes (Serafini-Fracassini and Del Duca 2008; Zhong et al. 2019).

The microbial TGases identified to date do not share a significant sequence similarity with any of the other characterized TGase classes. Their biological functions remain largely unknown, and they are essentially unstudied beyond their early identification (Giordano and Facchiano 2019; Makarova et al. 1999). An in silico study by Makarova et al. (1999) identified a class of microbial proteins with only one characterized member—a single protease that shares a significant sequence similarity with animal TGases. They thus proposed papain-like thiol proteases as common ancestors of all TGases.

The first oomycete TGase to be characterized was found thanks to its role in the induction of immune responses in plants. A 42 kDa cell wall glycoprotein (GP42) of *Phytophthora sojae*, previously shown to contain the 13 amino acid peptide (Pep13) that acts as an elicitor of defense mechanisms in parsley (Hahlbrock et al. 1995; Nürnberger et al. 1994), was characterized as a Ca^{2+}-dependent TGase, and its homologs were found in all *Phytophthora* species, including *P. infestans* (Brunner et al. 2002). Although the GP42 protein showed enzymatic and biochemical similarities to human TGases, its folding patterns were shown to be novel and not to resemble any characterized proteins (Reiss et al. 2011).

We have previously shown that peptides from the putative TGase encoded by the *P. infestans* gene *PITG_22117* are found predominantly in the cell wall of germinated cysts and penetration structures (Grenville-Briggs et al. 2010). Oomycete penetration structures resemble fungal appressoria and thus have previously been referred

to as appressoria or appressoria-like structures. Recently, they have also been described as knife-like structures (Bronkhorst et al. 2021) with sharpened edges to aid in penetration of the plant cuticle. It is suggested that these specialized structures be called naifu appressoria (Evangelisti and Govers 2024) to distinguish them from fungal appressoria. For simplicity, we will refer to these as appressoria throughout this article. The *PITG_22117* gene is highly expressed in cysts and appressoria and during the early stages of infection of potato plants (Grenville-Briggs et al. 2010; Resjö et al. 2017). These results suggest a role for TGases in the development of infectious structures and hence the pathogenicity of *P. infestans*. To test this hypothesis, in the current study, we performed an in silico analysis of the putative TGase family in *P. infestans*. We identified six additional putative genes and transiently silenced all seven of them to screen for possible developmental changes due to the lack of putative TGase expression. Silencing resulted in structural changes in appressoria, the formation of which correlated with a reduction in pathogenicity. Similar phenotypes were observed upon treatment of *P. infestans* cysts with the TGase inhibitor cystamine.

Materials and Methods

In silico analysis and phylogenetics

The DNA sequence of the *P. infestans* gene *PITG_22117* retrieved from the National Center for Biotechnology Information (NCBI; gene ID 9468508) was used to search for similar sequences in *P. infestans* using BLASTn. Alignment of the sequences was performed using Clustal Omega (Madeira et al. 2019; Supplementary File S1). The translated *PITG_22117* sequence was used in extensive BLASTp searches against different kingdoms, phyla, and genera. To identify any additional proteins not found by BLAST and predicted to have TGase function, a string search, "*Phytophthora infestans* transglutaminase," was used to search the NCBI Gene database. For all 21 results, the protein sequences were retrieved from the database and used to construct a maximum likelihood phylogenetic tree (highest log likelihood and bootstrap method with 1,000 replications) using MEGA11 software (Tamura et al. 2021). The functional domain and signal peptide predictions were performed using InterProScan (Jones et al. 2014), and protein folding and structure were predicted using Phyre2 (Kelley et al. 2015) and AlphaFold (Jumper et al. 2021; Varadi et al. 2022) tools.

Cultivation of *P. infestans*

All experiments were carried out using *P. infestans* strain 88069. For maintenance, cultures were grown on solid rye sucrose medium (Caten and Jinks 1968) at 18°C in darkness and sub-cultured every 2 to 3 weeks. Liquid cultures for extraction of RNA and growth inhibition assays were grown in pea broth, pH 7.25, at 18°C in darkness.

Transglutaminase expression throughout the life cycle of *P. infestans* and infection time course

To analyze the expression profiles of all the investigated TGases, 14-day-old cultures were grown on rye sucrose, and sporangia, zoospores, cysts, germinated cysts, and appressoria were collected as described previously (Grenville-Briggs et al. 2010; Resjö et al. 2017). The samples were collected from pooled material originating from 20 individual cultures. The collected cysts were used to inoculate potato leaves (cultivar Désirée) in a detached leaf assay, and infection time point samples were collected at 6, 12, and 24 h postinoculation (hpi). Mycelium samples were grown in liquid pea medium for 48 h before collection. Each sample was ground in liquid nitrogen, and the total RNA was extracted using the Qiagen RNeasy Plant Mini kit following the manufacturer's protocol. The samples were DNase-treated (Turbo DNA-free Kit, Invitrogen) before first-strand cDNA synthesis was performed as described (SuperScript III, Invitrogen; Grenville-Briggs et al. 2010). The life-cycle-stage cDNA samples were diluted to 5 ng μl^{-1} and the infection samples to 20 ng μl^{-1} before gene expression analysis by qRT-PCR. The qRT-PCR was performed in a Bio-Rad real-time PCR cycler using SYBR green as the fluorescent dye and specific primer pairs (Table 1). The analysis was run three times with three to four technical replicates per sample. The expression of TGase genes was normalized to a reference gene, *Actin A*, and the mycelium was used as a calibrator sample with expression set to 1; the relative expression was calculated using the modified Delta-Delta Ct method, as described previously (Avrova et al. 2003).

RNA interference

Oligonucleotide primers with T7 polymerase RNA promoters (Table 1) were designed to amplify a 200-bp TGase amplicon. Due to high sequence similarity, it was not possible to design unique primers for each of the TGase genes; therefore, the designed primers were able to amplify fragments from seven similar TGase genes: *PITG_22117*, *PITG_16953*, *PITG_16956*, *PITG_16958*,

TABLE 1. Primer pair sequences used for qRT-PCR and double-stranded RNA synthesis[a]

Gene	Primer sequences	Amplicon size
PITG_22117	F: CAAGGTCTCGACTGTGTTCA	167 bp
	R: CATCAGCGACAAATGAATGC	
PITG_16956	F: ACGATCTCCAAATCGTCACC	150 bp
	R: CGTAGTCAAGTTGGCAAGCA	
PITG_16958	F: CGGAGCCTGTCTTCTCAAAG	153 bp
	R: AGTCCTTGGCGGACTTCTCT	
PITG_16959	F: GTTGGGATGACACGGCTATC	150 bp
	R: GCGTGTGAACAGCCTGAGTA	
PITG_16963	F: CCTGCCTACTAAGGGTGTGC	150 bp
	R: AAATCCGTCACGTCAAGACC	
PITG_16953	F: GATGCGTACACGACGACAAC	150 bp
	R: TGTGGTAGACGTCGAAGTGG	
PITG_08335	F: CATGGACATCAAAGCTCTCG	145 bp
	R: AGGATTCATGTCGCGGTAAG	
Actin A	F: CATCAAGGAGAAGCTGACGTACA	69 bp
	R: GACGACTCGGCGGCAG	
22117_T7	F: GTAATACGACTCACTATAGGGGTGCGAGGGTTCAAGGTGTA	142 bp
	R: GTAATACGACTCACTATAGGGCGAAGATCCACGAGAGACG	
	R2: GTAATACGACTCACTATAGGGGGTCGTGTAGCGATCAACCT	198 bp
GFP_T7	F: GTAATACGACTCACTATAGGGGCAGATTGCGTGGACAGGT	NA
	R: GTAATACGACTCACTATAGGGCTGGAGTACAACTACAACT	

[a] The underlined fragments of the double-stranded RNA synthesis primers correspond to the T7 promoter sequences. NA, not available.

PITG_16959, *PITG_16963*, and *PITG_08335*. Lack of binding elsewhere was confirmed by a BLASTn search within the *P. infestans* genome (performed with the low-complexity filter turned off). Double-stranded RNA (dsRNA) was synthesized with the MEGAscript RNA interference (RNAi) kit (Ambion) according to the manufacturer's protocol using 1 μg of the PCR product. Green fluorescent protein (GFP) was used as a non-endogenous positive control to ensure that any possible phenotypical changes arose from the silencing and not the transformation protocol. Preparation of protoplasts and introduction of the dsRNA were performed as described in Grenville-Briggs et al. (2008). Briefly, sporangia collected from five 10- to 14-day-old solid culture plates were transferred to 200 ml of pea broth medium and incubated at 20°C for 48 h, after which the germlings were harvested on a 40-μm mesh, washed twice with mannitol-magnesium sulfate buffer and incubated shaking for 60 to 90 min in protoplast solution. The protoplast solution consisted of 10 mg/liter of lysing enzymes (Sigma) and 5 mg/liter of cellulose (Sigma) dissolved in the mannitol-magnesium sulfate buffer. The solution was then filtered to remove any undigested mycelia, the protoplasts were collected by centrifugation at 600 × *g* for 5 min at 4°C, the supernatant was removed, and protoplasts re-suspended in 5 ml of mannitol-magnesium sulfate buffer. The wash was repeated four times, after which the protoplasts were counted, and the concentration was adjusted to 0.2 to 1.5×10^6 protoplasts/ml. For each dsRNA solution, 10 μl was mixed with 10 μl of Lipofectin solution (Invitrogen), incubated for 15 min at room temperature, and mixed gently with an equal volume of protoplast solution. To facilitate transfection, the protoplast-dsRNA mixture was incubated for 16 to 18 h at 20°C, after which time the solution was gently mixed with 200 ml of pea broth and aliquoted into microtiter plates. After 3 days, newly formed single hyphae were transferred onto solid rye agar plates. Fourteen days after the transfection, zoospores were collected from single colony plates and encysted. A small portion (about 200 μl) of each of the samples was used for detached leaf assays and gene expression analysis, and the remainder was incubated in plastic Petri dishes at 11°C in darkness for 16 h to induce cyst germination and appressoria structure formation. The numbers of germinated cysts, appressoria, and any aberrant structures were counted using an inverted light microscope. The silenced lines were compared with the GFP control lines.

Assessment of virulence of *P. infestans* RNAi lines

The virulence of the RNAi lines was assessed by detached leaf assays (DLAs). Healthy leaves of similar size were removed from the middle of the potato plant and placed abaxial side up in plastic boxes lined with moist paper tissue to ensure high humidity levels were maintained. Each leaf was inoculated with four 10-μl droplets of cyst solution (50,000 cysts/ml) from a single RNAi line on one side of the leaf and four 10-μl drops of the GFP-control cysts (50,000 cysts/ml) on the other side of the leaf. There were four leaves inoculated for each RNAi line, two for visual assessment of pathogenicity and two for material collection for gene expression analysis (see next section). The boxes were sealed with parafilm and placed in climate chambers with a cycle of 16 h of light and 8 h of darkness at 18°C, starting with the dark period, as described in Resjö et al. (2017). The symptoms were compared at 4 and 7 days postinoculation. Visual observations were complemented by leaf scans performed in Bio-Rad ChemiDoc MP Imager using a low-light fluorescence Cy7 filter (transmission between 755 and 777 nm; exposure time 5 s) to visualize the dead tissue (Zahid et al. 2021).

TGase expression in the RNAi lines

To ensure sufficient material for the gene expression analysis, cysts produced from the RNAi lines were used to inoculate potato leaves (as described in the previous section). Eight leaf discs per sample were collected at 6 hpi and snap-frozen in liquid nitrogen. The cork borer and forceps used for sample collection were washed with 70% ethanol between different lines. The RNA extraction and qRT-PCR analyses were performed as described above, using specific primers (Table 1).

Effect of TGase inhibitor cystamine on *P. infestans* growth and pathogenicity

To test the effect of cystamine on *P. infestans* growth, a liquid medium with varying concentrations of cystamine ranging from 0.5 to 25 mM was inoculated with small plugs of a solid agar culture that were excised with a cork borer to ensure the same size for all cultures. The growth differences were estimated daily (using a school ruler) until the control culture reached the edges of the Petri dish. To test if the effects of the drug were reversible, the cultures containing cystamine were left in the incubator for 14 days. Additionally, cystamine in concentrations of the same range (0.5 to 25 mM) was added to a solid rye sucrose medium, and the cultures were grown until the radial growth of the control cultures reached the edge of the Petri dish. Solid cultures with cystamine in the medium were then used to test the effect of the drug on sporulation. The plates were flooded with sterilized tap water, and sporangia were collected and counted using a hemocytometer.

To investigate the effects of cystamine on zoospore release and motility, 12- to 14-day-old cultures were flooded with either water or cystamine solutions at varying concentrations ranging between 25 and 200 mM (based on the results of growth assays) and incubated at 4°C for 4 h, after which zoospores were harvested, filtered through a 40-μm mesh, and counted. Encystment was induced as described previously (Resjö et al. 2017), and samples were incubated for 2 to 4 h at 20°C, after which cyst germination was evaluated by light microscopy. Alternatively, to assess the rate of cyst germination, 12- to 14-day-old cultures were flooded with water, incubated at 4°C to release zoospores, filtered, and encysted. The cysts were collected by centrifugation (1,200 × *g*, 15 min), the supernatant was removed, and cysts were re-suspended in either fresh water (controls) or cystamine solution. Germination was assessed as described above, after 2 to 4 h of incubation at 20°C.

Finally, to assess formation of appressoria, cysts were induced as described above, either in the presence of cystamine or treated with cystamine after encystment, and incubated for 16 h at 11°C in Petri dishes. Control samples were encysted as described and then treated with water. The numbers of cysts, germinated cysts, appressoria, and any aberrant structures were counted using an inverted light microscope.

The effect of the cystamine treatment on *P. infestans* pathogenicity was tested with a DLA as described above for RNAi. The leaves were inoculated with two droplets each containing 50,000 cystamine-treated cysts on the left of the central vein and on the right side with a water-treated control cysts and additionally with just cystamine to test the effect of the drug on the potato leaf.

TGase gene expression in cystamine-treated cysts

Leaf disc samples were collected at the inoculation site of the DLA (described above) at 6 hpi. Each sample consisted of eight leaf discs collected from three leaves. The RNA extraction, DNase treatment, cDNA synthesis, and qRT-PCR were performed as described above.

Effect of cystamine on turgor pressure of appressoria

The turgor pressure of the appressoria was measured indirectly by counting the number of collapsed appressoria in various concentrations of PEG8000 using an incipient cytorrhysis assay (Howard et al. 1991; Michel 1983). These concentrations covered a range of osmotic pressures, which were represented using a standard curve. The turgor pressure of the cell is estimated to be equal to the pressure at which 50% of appressoria collapse, indicating cytorrhysis. The graph and calculations were performed using GraphPad Prism 8.2.1

and a standard curve interpolation. Separate curves were drawn for samples with and without cystamine.

TGase enzymatic activity assay

Eighty agar cultures of *P. infestans* were used to collect sufficient material for cell wall protein extraction. Forty plates were used to collect sporangia and 40 for cysts. Sporangia cultures were flooded with 5 mM cystamine in water or just water (20 cultures each), incubated for 3 to 4 h at room temperature, and collected as described previously (Grenville-Briggs et al. 2010; Resjö et al. 2017). The cultures for cyst collection were flooded with 2.5 mM cystamine or water (20 cultures each) and incubated for 2 h at 4°C, after which the cysts were collected as described previously (Grenville-Briggs et al. 2010; Resjö et al. 2017). All samples were snap-frozen in liquid nitrogen, ground using sterile micropestles, suspended (without allowing them to thaw) in at least 200 µl of Tris-HCl (pH 7.5) and 10 µl of protease inhibitor cocktail (P9599), and vortexed vigorously. An equal volume of 1 M NaCl was then added, and the samples were centrifuged for 5 min at 7,000 rpm, at 12°C. The supernatant containing intracellular proteins was removed, and the pellet was washed with NaCl and then processed according to the Abcam Transglutaminase Activity Kit (Abcam ab204700), including the addition of the homogenization buffer with dithiothreitol. The tissue homogenization step was omitted. The absorbance was measured at 525 nm, and the TGase activity of the samples was estimated based on the standard curve. Data correction and calculations were done according to the manufacturer's guidelines.

Birefringence

To analyze the effect of cystamine treatment on the structure of the cell wall of cysts and appressoria structures, 12- to 14-day-old cultures of *P. infestans* were flooded with water, incubated at 4°C to release zoospores, filtered, and encysted. The cysts were collected by centrifugation (1,200 × *g*, 15 min), the supernatant was removed, and cysts were re-suspended in either fresh water (negative controls), 2,6-dichlorobenzonitrile (DCB; positive controls), or cystamine solution. The birefringence of the cell wall of cysts was examined with polarized light microscopy (Leica DMLB microscope, 20× PH objective and Leica Polarizer L ICT/P set at 90 degrees with similar light intensity) after 3 to 4 h of incubation at 22°C. The formation of appressoria was induced, as described above, by 16 h of incubation at 11°C. Images were captured using a DCF450 camera and LAS core software system with a 250-ms exposure time and gamma of 1. The images were then analyzed using ImageJ (NIH) software with the background pixel intensity normalized to 100. The average pixel intensity was then calculated based on the segmented line tool, starting at one end of a cell wall, crossing over at roughly the halfway point, and passing back over the cell wall, completing at the end of the cell wall. Two measurements were taken for each analyzed structure, at opposing ends of the cell. The background average pixel intensity near the cell wall was subtracted from the average pixel intensity values of the cell wall to achieve the birefringence value.

Results

There are 21 putative TGases identified in *P. infestans*

In previous studies, at least one *P. infestans* TGase protein was found in the cell wall of germinating cysts and appressoria (Grenville-Briggs et al. 2010). Furthermore, it was verified that the *PITG_22117* gene encoding this protein is highly expressed in cysts and appressoria and at early infection stages (6 and 12 hpi) when the appressoria are formed on the leaf surface and start to penetrate the host cells (Resjö et al. 2017). The current study used an in silico approach to look for other TGases using sequence similarity searches. A BLASTn search yielded five additional genes, two of which belong to the M81 gene family: *PITG_16956*, *PITG_16958*, *PITG_16959* (*M81D*), *PITG_16963* (*M81C*), *PITG_22104*, and one gene labeled just as *M81E*. Sequence similarity searches (BLASTn) using all six sequences yielded no results outside of the *Phytophthora* genus, and within the genus, peptides from only five other species produced significant alignments (*P. parasitica*, *P. plurivora*, *P. agathidicida*, *P. sojae*, and *P. capsici*). Protein BLAST (BLASTp) searches showed moderate to high similarity (50 to 75% identity) to peptides from other oomycetes, moderate similarity (40 to 50%) to fungi from genera *Catenaria* and *Quaeritorhiza*, and low similarity (<40%) to other fungi and bacteria.

String searches, such as "*Phytophthora infestans* transglutaminase," using the NCBI non-redundant gene database found 21 results with varying degrees of annotation. The protein sequences of all these 21 genes were retrieved and used to construct a maximum likelihood phylogenetic tree (Supplementary Fig. S1). The phylogenetic analysis of the protein sequences confirmed that proteins encoded by the genes found by BLASTn group together. From the phylogenetic analysis, two additional genes of high sequence similarity, *PITG_16953* and *PITG_08335*, were also identified. Moreover, with the exception of *PITG_22104*, which is a short sequence with 100% similarity to *PITG_16959* and thus a possible pseudogene, all of the six genes with high similarity to *PITG_22117* include the conserved sequence encoding the Pep13 peptide, an elicitor of plant defense responses (Brunner et al. 2002; Nürnberger et al. 1994). The *PITG_22104* gene was excluded from further analysis.

The gene model for *PITG_22117* from the Joint Genome Institute Genome Portal shows that this gene is located on a small contig of the *P. infestans* isolate T30-4 genome, and the available sequence is possibly truncated. It was also not found in the recent chromosome-level genome assembly of isolate 1306 (Matson et al. 2022), suggesting that it could be a copy of the gene *PITG_16956* with which it shares the highest sequence similarity. However, sequence alignment of these two genes shows that the length is not the only difference between the two sequences, and there is a substantial number of mismatched nucleotides between them. Therefore, despite the fact that the *PITG_22117* genomic sequence might not be complete, and given that the current study used isolate 88069, *PITG_22117* was treated as a separate gene.

All Pep13 TGases are elicitor proteins

The seven TGases containing the Pep13 peptide were functionally annotated in silico. The presence of a TGase elicitor domain (IPR032048) was predicted in all of them. Additionally, in all seven proteins, the TGase domain overlapped largely with a MANSC (motif at N terminus with seven cysteine domains; PTHR16021) (Fig. 1). The presence of transmembrane helices was predicted with transmembrane topology prediction software in proteins encoded by genes *PITG_16956*, *PITG_16958*, *PITG_16959*, and *PITG_16953*. All these proteins were also predicted to contain signal peptides at their N-termini. The regions of the proteins not covered by these functional domains were predicted as non-cytoplasmic domains, with the exception of a protein encoded by gene *PITG_16963* that contains a stretch of 185 amino acids at its N-terminus for which there were no domains predicted. Protein folding predictions with Phyre2 showed only very weak alignment with known protein models, with model confidence levels ranging from 2.7 to 34.8%. In most of the predictions, the highest scoring model was annotated as a membrane protein. Using AlphaFold allowed us to predict the structure of *PITG_22117* and *PITG_08335* with a high degree of certainty (70 to 90% model confidence), but the remaining five proteins contained regions of uncertainty (Fig. 1). The uncertainty regions may occur due to intrinsic disorder, or, alternatively, may represent errors in either sequencing or protein predictions. However, in each of these proteins, the regions containing the predicted TGase domains have clearly predicted organized structures.

The elicitor TGases are highly expressed at early infection time points

The expression of all seven elicitor TGase genes was compared in the asexual pre-infection stages (produced in vitro) and early infection time points (detached leaf assays) sampled at 6, 12, and 24 hpi (Fig. 2). Because the infection of the potato leaves was accomplished with a droplet of cyst solution, the samples collected in this assay contained little *P. infestans* material compared with plant one, and especially the 6 hpi sample, where the cysts had just started germinating and did not produce a lot of biomass. For that reason, the detection of *P. infestans* genes in the infection samples was comparatively more difficult than in the life cycle stages, and the standard deviation between the technical replicates in the qRT-PCR analysis was higher, yielding larger errors. Nonetheless, the obtained results are a strong indication of a trend in gene expression in these samples. Expression of *PITG_16958* was undetectable in either in vitro or infection assays. Of the six remaining genes, five showed the highest expression at the 6 hpi time point. *PITG_22117* was the only gene in which no significant differences were found between the different pre-infection life cycle stages, and *PITG_16953* was the only gene in which the expression was the highest in the zoospores. A comparison of only the life cycle stages shows that three genes, *PITG_16959*, *PITG_16963*, and *PITG_16953*, were expressed the most in the zoospores. *PITG_08335* also exhibited higher expression in the zoospores, but the induction was only slight and much lower than in the other three genes (Fig. 2). There was no signal read for this gene in appressoria or at 12 and 24 hpi, indicating an absolute lack of expression during these stages considering three independent biological replicates. *PITG_16956* showed a more specific expression pattern being highly induced in the germinated cysts. Nonetheless, the level of induction was generally much lower in this gene than in the zoospore-specific ones (Fig. 2).

Chemical inhibition of TGases affects the growth and germination of *P. infestans*

Cystamine was previously reported to inhibit the activity of TGases in humans (Jeitner et al. 2018; Lorand and Graham 2003) and fungi (Iranzo et al. 2002; Ruiz-Herrera et al. 1995). Cystamine treatment of fungi resulted in growth inhibition and morphological changes, influenced incorporation of peptides into the cell wall, and inhibited the yeast-to-mycelium transition in dimorphic fungi (Reyna-Beltrán et al. 2019). However, the effects of cystamine on oomycete growth or development have not been tested before. *P. infestans* was grown in both liquid and solid media at a range of cystamine concentrations, and independent of the type of medium, 5 mM cystamine inhibited mycelial growth by about 40%, 7.5 mM by 60%, and 10 mM by 90%, and at 20 mM and higher concentrations, there was no growth observed at all. Sporangial germination was also affected by the chemical treatment: 7.5 mM cystamine inhibited germination completely, whereas at 5 mM cystamine, there were only single germ tubes found. The germ tubes at 2.5 and 1 mM cystamine had more deformations than the ones seen at lower concentrations (Fig. 3). To test the effect of cystamine on zoospore release, solid cultures were flooded with cystamine solutions of concentrations ranging between 0.5 and 200 mM. None of the concentrations had any effect on the release or motility of the zoospores. However, cysts produced from cystamine-treated zoospores had a lower germination rate than untreated ones (Fig. 4A). At 0.5 mM, the germination rate was about 50% lower, whereas at 2.5 mM, it decreased by 75%. Interestingly, there were no differences in the rate of germination observed for cystamine concentrations ranging from 2.5 to 10 mM (Fig. 4A).

The number of appressoria formed was reduced significantly from about 35% of all structures in untreated samples to about 5% in those treated with 0.25 and 0.5 mM cystamine. Appressoria formation was severely inhibited by 2.5 mM cystamine (Fig. 4A), and the few appressoria that were produced were severely deformed, collapsed, or burst (Fig. 4B). Cysts treated with cystamine at concentrations higher than 1 mM lost pathogenicity, and there were no lesions observed at the site of inoculation on potato leaves under these conditions (Fig. 5A and B). Cysts treated with 1 and 0.5 mM cystamine produced smaller lesions than the control ones (Fig. 5B), and there was no mycelial growth on the surface of the leaf at the site of inoculation (Fig. 5A and B). It was verified that the cystamine itself did not have any visual effect on the leaflets and hence that the observed tissue damage was solely due to the pathogen infection.

Finally, cystamine was tested for effects on protoplast recovery. Protoplasts were made by treatment of liquid-grown mycelia with

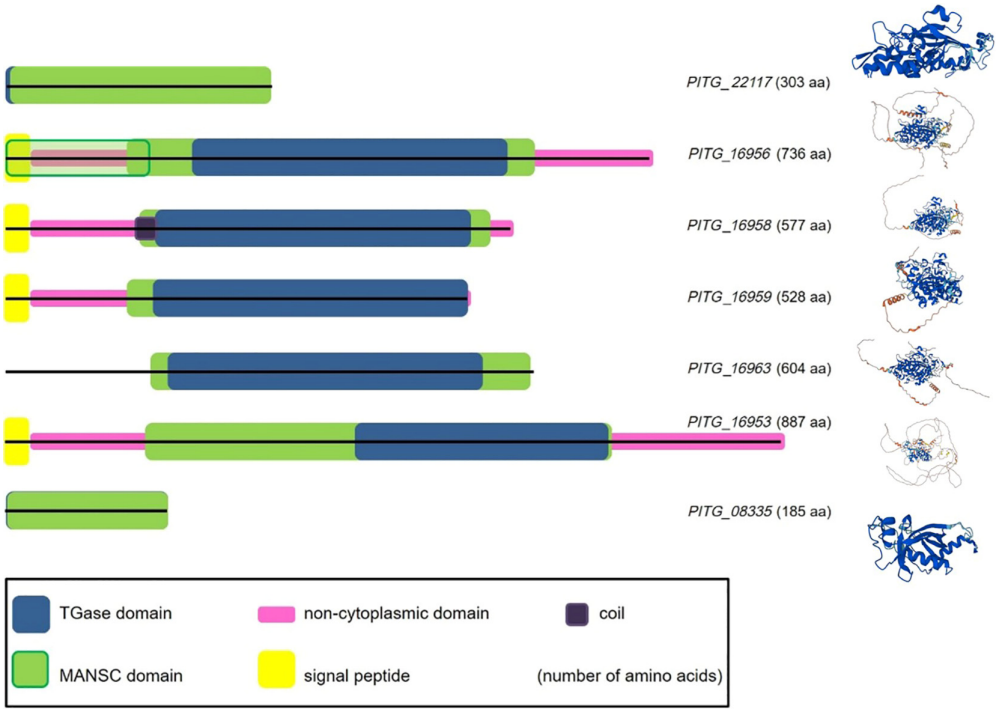

Fig. 1. Putative functional domains in elicitor transglutaminases (TGases) and their predicted structures. The sequences were aligned at amino acid (aa) 1 to show the difference in length. Functional domains predicted by InterProScan are represented by blocks of different colors and drawn to scale (see legend at the bottom of the figure). AlphaFold structural predictions are shown to the right of each domain cartoon. Dark blue areas represent structural predictions with a high level of certainty, whereas red areas have a low certainty of prediction. Areas without structural predictions or that represent areas of intrinsic disorder are marked in gray.

lysing enzymes and cellulase. In line with previous findings in the true fungi (Ruiz-Herrera et al. 1995), treatment with cystamine delayed the recovery of protoplasts. The first emergence of germ tubes was observed after about 36 h in samples treated with cystamine, whereas in the wild-type protoplasts, recovery and germination were observed much earlier at about 24 h (data not shown). This effect was observed in samples treated with 5 and 2.5 mM cystamine but not in lower concentrations of the drug, which corresponds well with the reduction of the germination rate and increase in structural abnormalities in sporangia and cysts treated with cystamine.

Mycelial cell wall extracts from *P. infestans* exhibit TGase enzymatic activity

Despite sequence and structural differences between the *P. infestans* and human TGases, TGase enzymatic activity in cell wall protein extracts of *P. infestans* sporangia and cysts was demonstrated when tested with a kit designed for human TGases described above. The enzymatic activity in the *P. infestans* samples was lower than would be expected for human tissue samples, yet it was significantly above the detection levels of the kit, confirming the presence of TGases in the cell wall protein extracts. Furthermore, treatment with 2.5 mM cystamine significantly decreased the enzymatic activity of proteins extracted from the cell walls of cysts, confirming the suitability of cystamine as an inhibitor of TGase function (Supplementary Fig. S2).

Inhibition of TGases reduces the turgor pressure of appressoria

Because appressoria bursting and cell collapse were observed when *P. infestans* was treated with cystamine in vitro, the difference in turgor pressure produced in treated and untreated appressoria, using an incipient cytorrhysis cell-collapse assay, was measured. The untreated healthy appressoria exhibited an average turgor pressure of 3.3 MPa, whereas in appressoria produced in the presence of cystamine, the turgor pressure was estimated to be 1.3 MPa at 0.25 and 0.50 mM cystamine (Fig. 6).

Cystamine treatment of cysts and appressoria reduces birefringence of their cell wall in a manner similar to DCB

Birefringence (double refraction) has been widely used to study the cytoskeleton, including cellulose deposition and orientation in plant cell walls (Abraham and Elbaum 2013; Bischoff et al. 2010; Cranston and Gray 2008; Katoh et al. 1999). This method was therefore used to visualize differences in *P. infestans* cell walls after chemical inhibition of either cellulose synthesis or TGase activity. The birefringence of an intact cell wall in cysts and appressoria was compared with the birefringence of the same structures treated with either DCB, a known inhibitor of cellulose synthesis (Grenville-Briggs et al. 2008), or cystamine. Treatment with DCB had a similar effect on *P. infestans* cysts and appressoria as on plant cells, and the effective concentrations of DCB were very similar to the ones used in plants (Fig. 7A). The birefringence of the cell wall decreased as the concentrations of the cystamine increased (Fig. 7B). The appressoria were much more sensitive to the treatments than cysts, and particularly to cystamine, where the reduction of birefringence was more rapid, as seen by the larger slope of the curve.

RNAi-based transient silencing of TGases can be lethal

To confirm the importance of the elicitor TGases for the viability and development of cysts and appressoria structures in *P. infestans*, the TGase elicitor genes were transiently silenced

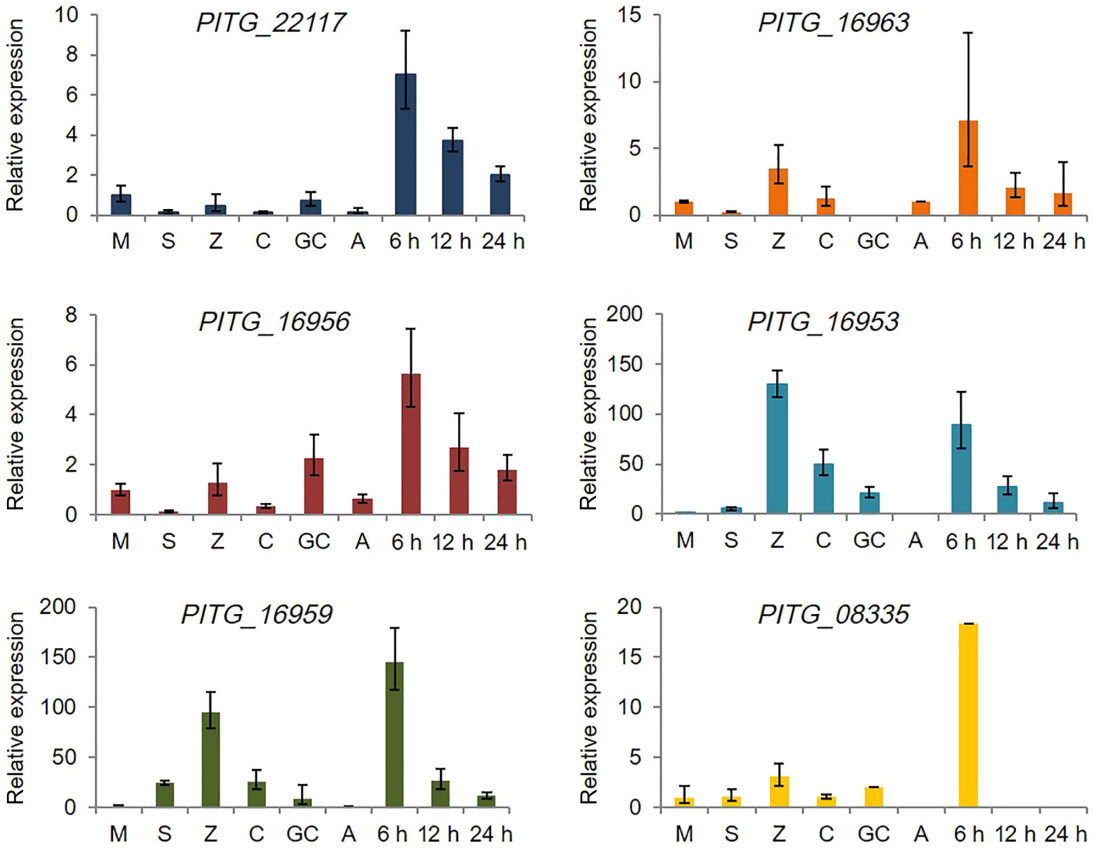

Fig. 2. Expression profiles of the elicitor transglutaminases. The expression was calculated relative to *Actin A* and calibrated to the mycelium sample for which the expression was set to 1. M, mycelium; S, sporangia; Z, zoospores; C, cysts; GC, germinated cysts; A, appressoria; 6, 12, and 24 h, h postinoculation with cyst solution on potato leaves. Gene *PITG_16958* is not shown, as there was no signal detected for this gene. Error bars represent errors calculated using the modified Delta-Delta Ct method. The RT-PCR was performed three times with three to four technical replicates per sample.

using RNAi. Primers were designed to amplify dsRNA molecules that recognize seven of the investigated genes (due to sequence similarity, the *PITG_16958* gene that showed lack of expression was also targeted). These genes exhibit such high sequence similarity that it was not possible to target them individually with RNAi. Silencing of the entire family of TGases proved lethal, and we could not recover the silenced lines. Given that the high level of sequence conservation prohibits silencing of individual genes, we redesigned the reverse primer to lower its specificity in an attempt to achieve less-efficient gene silencing. The new reverse primer matched genes *PITG_22117* and *PITG_16956* 100% but not the other ones. The match with *PITG_16958* was still high enough (3-nt mismatch) to ensure its silencing, whereas the sequence similarity with genes *PITG_16959*, *PITG_16963*, *PITG_16953*, and *PITG_08335* was much lower. This lower primer specificity allowed us to recover lines with intermediate phenotypes and varying expression levels of the targeted TGase genes (Table 1; Supplementary Fig. S3). The most severe phenotype seen was still lethal, with all of the structures either burst or bursting at the time of phenotype assessment (Fig. 8B). Several lines (2, 9, 12, 15, and 17) displayed phenotypes comparable to the control lines, with almost all cysts germinating and about 40 to 50% of them producing appressoria with only a few abnormal structures (Fig. 8A). Most lines with intermediate phenotypes displayed more structural abnormalities than the control lines (Fig. 8A), mostly swelling of the germ tubes (Fig. 8B) but also twisted and very long germ tubes or multiple germ tubes originating from the same cyst (Fig. 8B). Structures previously referred to as "appressoria like" were also observed (Grenville-Briggs et al. 2008; where what we now refer to as an appressorium-like structure was simply called an appressorium)—a bulging of the germ tube in an attempt to form an appressorium that fails and the germ tube growth continues (Fig. 8B). Finally, in some of the intermediate phenotypes, although there were not many abnormalities observed, there were fewer appressoria produced compared with the non-endogenous control lines (Fig. 8A). These phenotypes were similar to, and consistent with, those seen with cystamine treatment and described above. All RNAi lines that displayed phenotypic differences compared with the control lines had an overall lower level of TGase gene expression (Table 2; Supplementary Fig. S3). Two lines with higher numbers of abnormal structures (lines 3 and 7), two lines in which there were fewer appressoria produced but not many abnormalities (10 and 11), and two lines with a wild-type phenotype (9 and 12) were selected. As predicted from the expression profiles in the life cycle stages and infection time points (Fig. 2), *PITG_16958* was not expressed in any of the samples. In line 3, the remaining six genes were expressed at lower levels compared with control lines, and in line 7, four genes showed lower expression and two showed expression levels similar to, or higher than, the control lines (Table 2; Supplementary Fig. S3). In the lines with fewer appressoria structures, the overall expression was also lower than in the control sample, with only one gene in line 11 and two in line 10 showing similar or slightly higher expression levels than the controls (Table 2; Supplementary Fig. S3). In the two lines that did not display phenotypic differences, the overall expression of TGases was higher than in the other RNAi lines, with three genes showing expression similar to, or higher than, control levels and three genes showing reduced expression in line 9, whereas in line 12, five out of six genes were expressed at control levels or higher (Table 2; Supplementary Fig. S3).

To test the pathogenicity and virulence of the RNAi lines, cysts were collected from the same lines that were used for phenotypic assessment. For DLAs, the same leaf was inoculated with cysts from

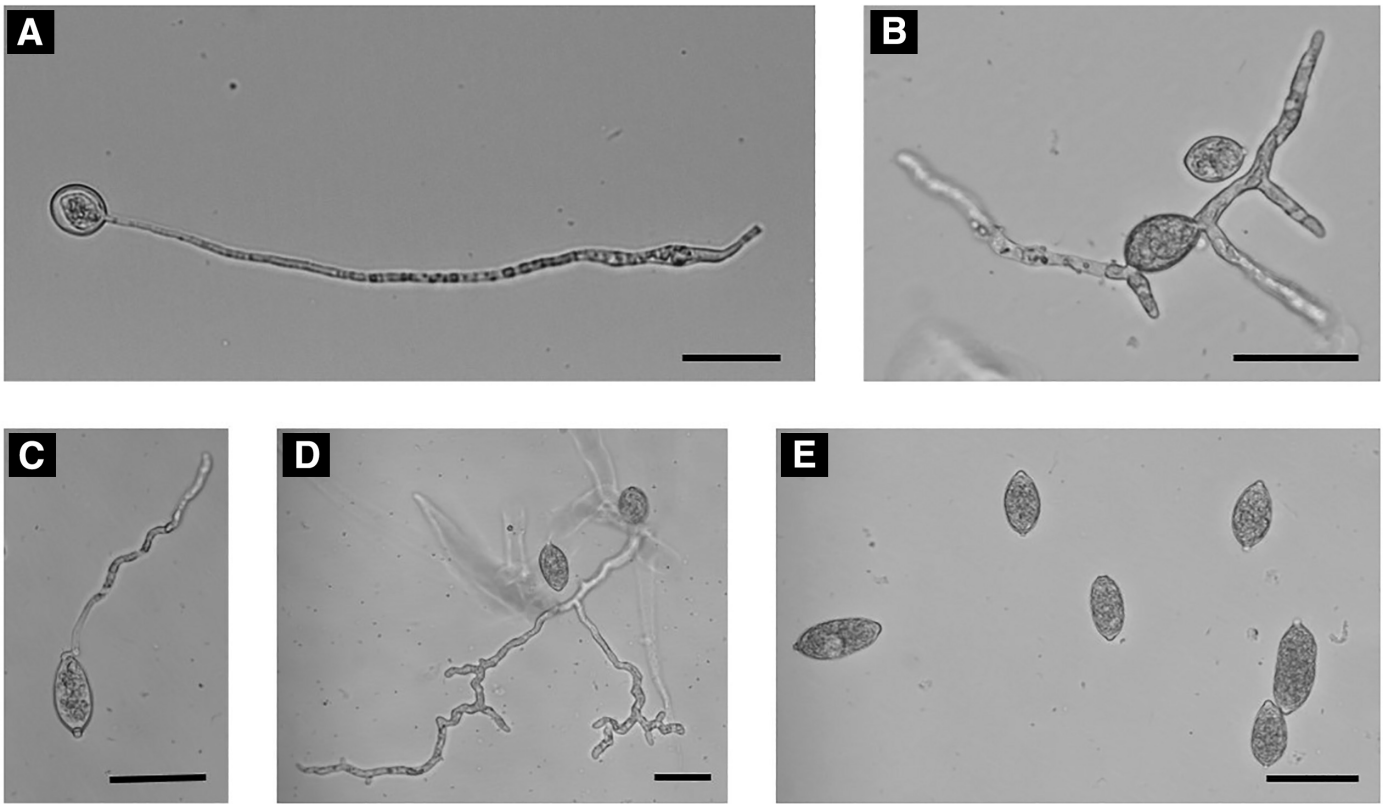

Fig. 3. Effect of cystamine on germination of sporangia. **A,** Untreated sample; **B,** 1 mM cystamine; **C,** 2.5 mM cystamine; **D,** 5 mM cystamine; and **E,** 7.5 mM cystamine. Panel A shows a germinating sporangium. Addition of cystamine to the growth medium resulted in B to D, deformations of the germ tubes; D, a lower percentage of germination; and E, at 7.5 mM, complete inhibition of germination. Scale bars = 50 μm. The experiment was repeated twice with five technical replicates per concentration of cystamine and with each sample originating from an individual culture (i.e., biologically independent material).

a single TGase RNAi line on the left side and from a single GFP non-endogenous control line on the right side of the primary vein to account for the possible adverse effects of the leaf detachment or minor variations in individual leaves. The majority of the TGase RNAi lines showed reduced virulence or no pathogenicity when compared with the control lines, including lines 3, 7, 10, and 11 (Fig. 8C) in which expression of TGase genes was overall lower than in the controls (Table 2; Supplementary Fig. S3). The virulence of lines 9 and 12 was not affected, which corresponds well with the gene expression data (Table 2; Supplementary Fig. S3). Similarly to the DLA conducted to look at the expression of the TGase genes, the samples collected from infected leaves contained little *P. infestans* material, and the product amplification in the qRT-PCR analysis occurred at later cycles, leading to higher variation between the replicates and thus higher errors. Therefore, the expression patterns in the silenced lines were treated with caution and used as complementary to the phenotyping and pathogenicity results.

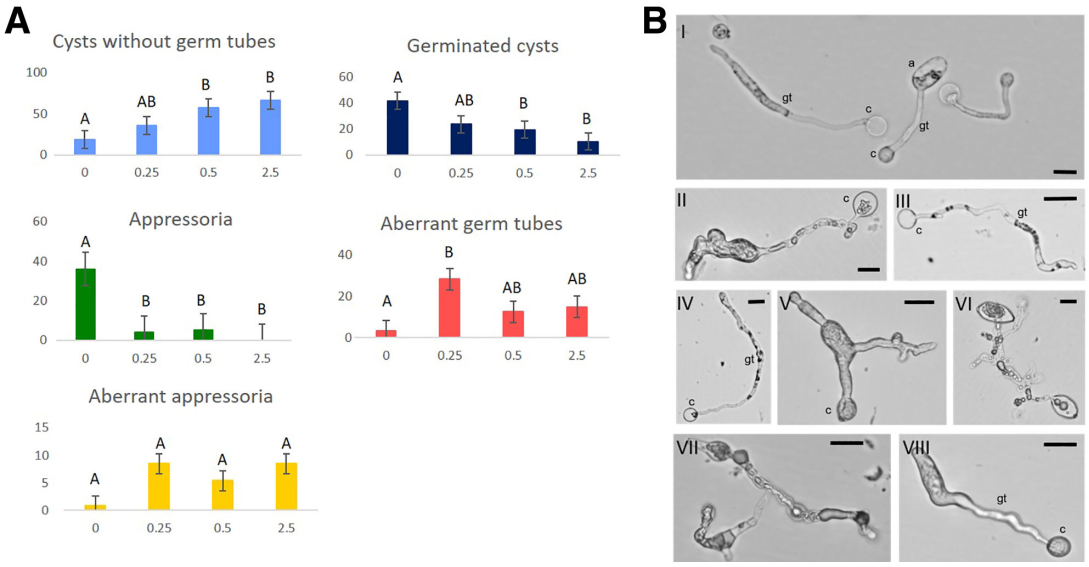

Fig. 4. Effect of cystamine treatment on cyst germination and formation of appressoria. **A,** The percentage of cysts, germinated cysts, appressoria, aberrant germ tubes, and abnormal appressoria was calculated for samples treated with different concentrations of cystamine. The error bars represent standard error, and the letters represent significance of the difference of means (analysis of variance followed by Fisher's least significant difference test). **B,** Inverted light microscope images of cysts treated with different concentrations of cystamine and allowed to form appressoria. I: Wild-type, untreated cysts (c) with healthy germ tubes (gt) and appressoria (a); II: cysts treated with 0.25 mM cystamine, about 50% germ tubes showed swelling and other deformations; III and IV: 0.5 mM cystamine, a large number of cysts germinated, but most of the germ tubes were deformed or collapsed; V and VI: 1 mM cystamine, severe deformations to germ tubes, in some cases making it difficult to discern particular structures; and VII and VIII: 2.5 mM cystamine, severe deformations like in 1 mM cystamine, very few appressoria, and the ones that formed were collapsed. Scale bars = 50 µm. The experiment was repeated five times with three to five technical replicates per concentration of cystamine and with each sample originating from an individual culture (i.e., biologically independent material).

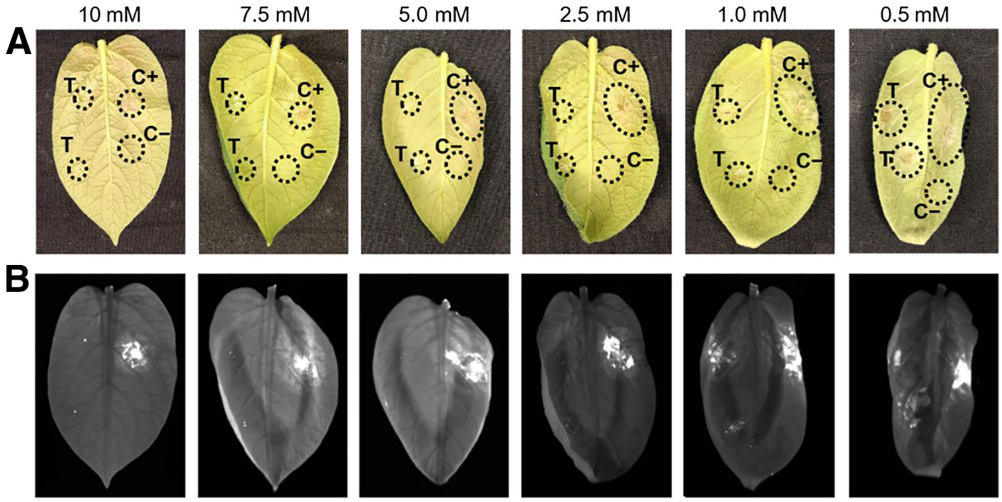

Fig. 5. Chemical inhibition of transglutaminases (TGases). **A,** Detached leaf assay (DLA). Potato leaflets were inoculated with two drops of cyst solution treated with cystamine of different concentrations (indicated above the pictures) on the left side of the leaf (T), with a control cyst solution in water on the top of the right leaf side (C+), and with just cystamine on the bottom right (C−). The same leaf was inoculated with the sample and both controls to screen for possible adverse effects of leaf detachment. Pictures were taken at 3 days postinoculation. **B,** DLA leaves scanned on ChemiDoc MP Imager with the Cy7 filter (transmission between 755 and 777 nm). Exposure time 5 s. The damaged areas of the leaflet appear bright in the image. Leaf wilting due to the time taken to process the images in the scanner might have caused slight differences in the leaf appearance between the A and B pictures. The DLA experiment was repeated three times with two technical replicates (two leaves) per concentration; each time, scans were taken for one of the experiments.

Discussion

In silico analysis of the *P. infestans* TGase gene family

The in silico analysis of *P. infestans* TGases showed that there are 21 TGases identified to date. Of these, the seven genes with the highest DNA sequence similarity to *PITG_22117*, a gene that encodes a protein localized to the cell wall, were grouped together in a phylogenetic analysis. Both DNA and amino acid sequence similarity searches showed that these genes and the proteins they encode are unique, with very little similarity to organisms outside the *Phytophthora* genus. In total, eight genes showed high sequence similarity and grouped together. Two of these genes were previously classified as members of the M81 gene family, and seven of them contain the Pep13 peptide. These findings are consistent with a study showing that the M81 gene family encodes elicitors, of which several are TGases containing Pep13 (Fabritius and Judelson 2003). Whereas the M81 protein was reported to be mating specific, other members of the family are expressed at different life cycle stages. A more recent study from the same group reported that one of the 21 putative TGases, *PITG_13497*, is induced over 100-fold during mating, where it is believed to play an important role in the synthesis of the very thick oospore cell wall (Niu et al. 2018).

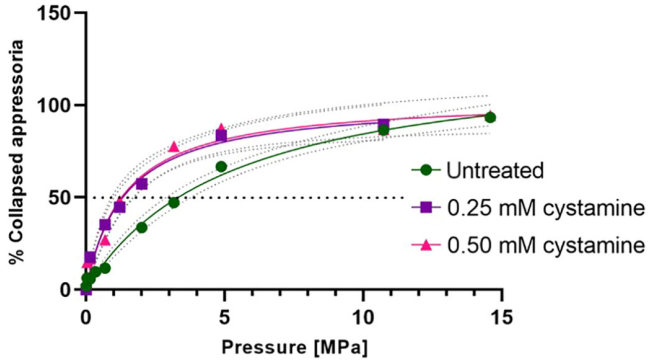

Sample	Turgor pressure
Untreated	3.3 MPa
0.25 mM cystamine	1.3 MPa
0.50 mM cystamine	1.3 MPa

Fig. 6. Effect of cystamine treatment on the turgor pressure of appressoria. Appressoria were incubated in different concentrations of PEG8000 and thus subjected to osmotic pressure ranging from 0 to 15 MPa. The graph presents interpolation curves. The turgor pressure of the cell is estimated to be the equal to the pressure at which 50% of appressoria collapse (cytorrhysis). The dotted curves represent the standard error for each of the interpolation curves. The experiment was repeated three times with two to six technical replicates per concentration of cystamine and with each sample originating from an individual culture (i.e., biologically independent material). The numerical values of turgor pressure for each sample are presented in the table below the graph.

Functional annotation of the Pep13-containing proteins confirmed that all of them are predicted to contain a TGase elicitor domain, as well as a MANSC domain. All animal proteins containing the MANSC domain that have been reported so far contain both signal peptide and transmembrane helix regions, and the seven cysteines are suggested to form disulfide bonds that play a role in protein structure and stability (Guo et al. 2004). However, of the seven proteins, only four were predicted to contain transmembrane helices and signal peptides. The lack of transmembrane helix or signal peptide prediction for the remaining proteins suggests that they may be entirely embedded in the cell wall or that they may be cytoplasmic or transported via non-classical secretion pathways. In the two shortest *P. infestans* proteins—*PITG_22117* and *PITG_08335*—the TGase and MANSC domains cover the entire length of their sequences, which may indicate that the available sequences that we used for the analysis are not complete. Nevertheless, the structures of these proteins were predicted with a high level of confidence by AlphaFold. Of the remaining five proteins, four were predicted to contain a non-cytoplasmic domain that covers their entire length, as well as areas of either intrinsic disorder or unclear structure, further supporting the hypothesis that they may be transported to the cell wall via non-classical secretion or alternatively suggesting that the model is not able to predict their structure very well. These predictions show that all seven members of this family are likely to be transmembrane proteins with putative TGase elicitor functions.

The pattern recognition receptor that binds Pep13 has recently been identified and cloned (Torres Ascurra et al. 2023). The confirmation that Pep13 is recognized by a surface receptor in potato further strengthens the hypothesis that Pep13-containing TGases are located in the cell wall of *P. infestans*, which would allow the peptide to be detected by this receptor.

Zoospore encystment requires expression of TGase genes

Analysis of the expression of the seven elicitor TGase genes in pre-infection stages and at early infection time points (6, 12, and 24 hpi) showed that the expression patterns vary between the different TGases. The *PITG_16958* gene was not expressed at all in any of the samples, suggesting that it might be expressed specifically in the sexual reproduction cycle or at only very low levels. A recent study of *P. infestans* sexual reproduction revealed that gene expression could be strain-dependent, and the level of expression during formation of the oospores can vary for different strain combinations, with *PITG_16958* highly upregulated in some of the strains and downregulated in others (Tzelepis et al. 2020; G. Tzelepis and K. P. Hodén, *personal communication* with the authors). It is also possible that *PITG_16958* is not expressed in the 88069 strain used in this study.

PITG_16953 was the only gene in which the expression was the highest in the zoospores, whereas in the remaining five genes, the highest expression was observed at 6 hpi on detached potato leaves (i.e., at the time point when the majority of appressoria are formed on the leaf surface). The much higher level of gene

TABLE 2. Relative expression of transglutaminase genes in RNA interference (RNAi) lines[a]

	Gene number						
RNAi line	*PITG_22117*	*PITG_16956*	*PITG_08335*	*PITG_16953*	*PITG_16959*	*PITG_16963*	Virulence
3	*	*	*	*	*	*	Lower
7	1.95	0.30	0.51	1.96	0.30	0.32	Lower
9	*	1.98	*	1.78	2.04	*	Full
10	0.89	0.33	0.60	1.67	1.10	*	Lower
11	1.06	0.57	*	0.93	0.70	0.30	Lower
12	5.91	2.41	2.30	0.97	2.93	1.58	Full

[a] The presented values are the expression relative to the expression of the reference *Actin A* gene and calibrated to the expression of the specific gene in the green fluorescent protein control sample, which was set to 1. Values above 1 indicate higher and below 1 indicate lower expression than the expression of the given gene in the control sample. * indicates lack of detected signal (i.e., the expression is below the detection level). Pathogenicity data from detached leaf assay experiments are presented for comparison.

expression at 6 hpi than in pre-infection stages indicates that the expression of the genes is not only life cycle specific but also induced by the presence of the host. This was the most pronounced in *PITG_22117*, where there were no significant differences found between the different pre-infection life cycle stages, and the expression was only induced by the infection. However, it needs to be pointed out that due to a low pathogen-to-plant material ratio, the results of the qRT-PCR analyses with infection samples are less reliable than those from life cycle stages, and all these data should be considered as trends rather than definitive expression values. Genes *PITG_16959*, *PITG_16963*, *PITG_16953*, and *PITG_08335* are most likely zoospore specific because their expression was significantly higher at this stage than in any other part of the life cycle tested. Because zoospores lack a cell wall and it is at the transition between the zoospore and cyst when the cell wall needs to be quickly formed de novo (Grenville-Briggs et al. 2008), the high level of gene expression points toward a role for these genes in cyst cell wall formation and possibly in the development of the (pre)infectious structures. Furthermore, *PITG_08335* was not expressed at all in appressoria and at 12 and 24 hpi, indicating a specialized role of the TGase encoded by this gene. Furthermore, the expression pattern of *PITG_16956* points toward a more specific function of the protein, as the gene was induced the most in the germinated cysts, when the germ tubes elongate rapidly and the appressoria are formed. However, the expression level of this gene was very low in all life cycle stages compared with the other genes. One hypothesis for this is that much higher levels of TGases may be necessary for the encystment and germination of cysts than for the formation of appressoria, and thus, several TGases are very highly expressed in the zoospores, whereas a lower induction is sufficient for the formation of appressoria.

Cystamine affects growth and development of *P. infestans*

Treatments with an inhibitor of TGase activity, cystamine, showed that the drug affects the development of all life cycle stages of *P. infestans* that require de novo cell wall synthesis. The growth of mycelia, germination of sporangia, encystment, cyst germination, and formation of appressoria were all affected, whereas even extremely high doses of the inhibitor did not have an effect on zoospore release or motility. Whereas the concentrations of cystamine required to inhibit mycelial growth and sporangia germination were rather high (20 and 7.5 mM, respectively), germination of cysts and formation of appressoria were severely affected at much lower doses. All germ tubes that formed in the presence of cystamine, independent of whether they originated from sporangia or cysts, showed an increasing number of abnormalities such as swelling, twisting, and extensive branching with the increasing drug concentration. Importantly, the rate of cyst germination decreased exponentially with the increasing cystamine concentration until it reached a plateau, and no further changes were observed between 2.5, 5, 7.5, and 10 mM. This suggests that germination may be only partially dependent on TGases or that not all *P. infestans* TGases are sensitive to this inhibitor. Because most of the TGases appear to be cell wall localized, the hypothesis that the ones without the signal peptide are entirely embedded in the cell wall structure may somewhat explain the latter hypothesis, as they may not be accessible to the drug due to their location and complex folding. It has been shown that cystamine undergoes a reversible reduction to cysteamine in vivo, and although the primary form in the extracellular compartments is cystamine, the cytosol environment facilitates conversion to cysteamine (Jeitner et al. 2018). The two drugs also for a mixed disulfide, and it is possible that this (larger and more complex) molecule cannot access the cell-wall-embedded TGases easily. An alternative might be that TGases are able to form complexes that protect their active sites from inhibition by this drug.

The reduced rate of appressoria formation and a high level of structural abnormalities observed in cystamine-treated samples also resulted in decreased pathogenicity. The cysts treated with concentrations higher than 1 mM cystamine (i.e., the concentration at which cyst germination was severely reduced and very few or no appressoria formed) were not able to infect potato leaves at all.

All these observations suggested that cystamine inhibited de novo cell wall formation, which was confirmed by delayed protoplast recovery in the presence of the drug.

Mycelial extracts from *P. infestans* exhibit TGase enzymatic activity

Retarded growth and development of *P. infestans* in the presence of cystamine does not, however, explicitly prove that the structural changes were caused by inhibition of TGases, as the drug could affect other proteins as well. Therefore, TGase enzymatic activity in cell wall extracts of sporangia and cysts was tested with or without cystamine. The results demonstrate that crude cell wall extracts of *P. infestans* possess TGase activity and that it was greatly reduced

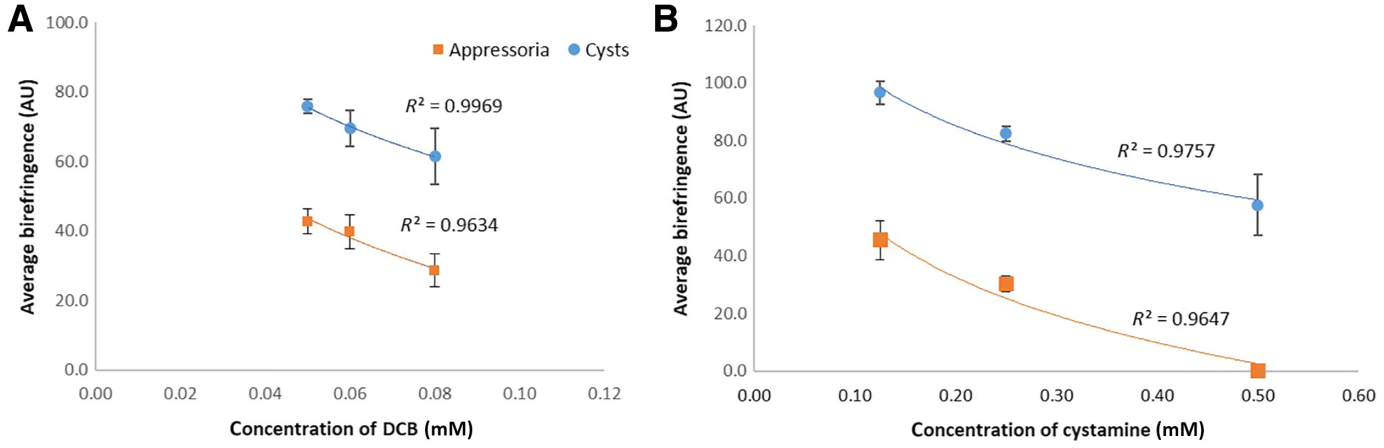

Fig. 7. Birefringence of cysts and appressoria. Average birefringence of cell walls of cysts and appressoria treated with **A,** 2,6-dichlorobenzonitrile (DCB) and **B,** cystamine. The birefringence was examined with polarized light microscopy (Leica DMLB microscope, 20× PH objective and Leica Polarizer L ICT/P set at 90 degrees with similar light intensity). Images were captured using a DCF450 camera and LAS core software system with a 250-ms exposure time and gamma of 1. The images were then analyzed using ImageJ (NIH) software. Two measurements were made for each analyzed structure, at opposing ends of the cell. The background average pixel intensity near the cell wall was subtracted from the average pixel intensity values of the cell wall to achieve birefringence value. The coefficient of determination is displayed directly next to the regression curves. The error bars represent the standard error. The experiment was repeated twice, and in total, there were 30 to 50 individual cysts and appressoria measured for each treatment.

by the presence of cystamine. Therefore, cystamine is confirmed to be a TGase inhibitor in *P. infestans*.

TGases are necessary for cell wall formation and rigidity

Appressoria are produced specifically to build pressure and to provide a focal point for the secretion of digestive enzymes to penetrate host cells. To break the barrier of the plant cell wall, appressoria must possess a thick cell wall and produce significant turgor pressure (i.e., the pressure resulting from plasma membrane being pushed against the cell wall) (Meng et al. 2009; Wang et al. 2005). To look further into the importance of TGases in the cell wall formation, we measured the turgor pressure (by an incipient cytorrhysis cell-collapse assay) and birefringence of cysts and appressoria with and without cystamine treatment. Both factors were affected by the presence of the drug. The average turgor pressure of appressoria decreased from 3.2 MPa in healthy cells to 1.3 MPa in the cystamine-treated samples. This is compared with the turgor pressure in the hyphae, which previous studies have estimated to be 0.6 to 0.8 MPa in fungi and 0.8 to 1.2 MPa in oomycetes (Brand 2012; Money 1990). This significant decrease in turgor pressure of cystamine-treated appressoria is in line with the finding that at this concentration, the virulence of the cysts is largely reduced and clearly demonstrates that an increase in appressorial turgor pressure is required for *P. infestans* infection.

Birefringence of the cysts and appressoria was also decreased by the treatment with cystamine. Because birefringence measurements are primarily used in studies of the cytoskeleton and cellulose deposition, the effects of cystamine were compared with the effects caused by the cellulose synthase inhibitor, DCB. In both cases, the birefringence of the cell walls decreased much more in the appressoria than in the cysts, indicating that the process of cell wall formation in the infectious structures is more complex and relies heavily on cellulose deposition and protein cross-linking. DCB treatment was previously shown to reduce birefringence of the cell wall in tracheary elements due to a decreased cellulose deposition (Taylor et al. 1992). A sharper decrease in birefringence observed in the cystamine treatment in comparison with DCB suggested that protein cross-linking may be particularly important for the production of the rigid and turgor-resistant cell walls of appressoria structures.

The role of TGases in *P. infestans* pathogenicity and development

To investigate the role of the TGases in the development of cysts and appressoria structures and in the pathogenicity of *P. infestans* in general, the entire family of elicitor TGases was silenced using an

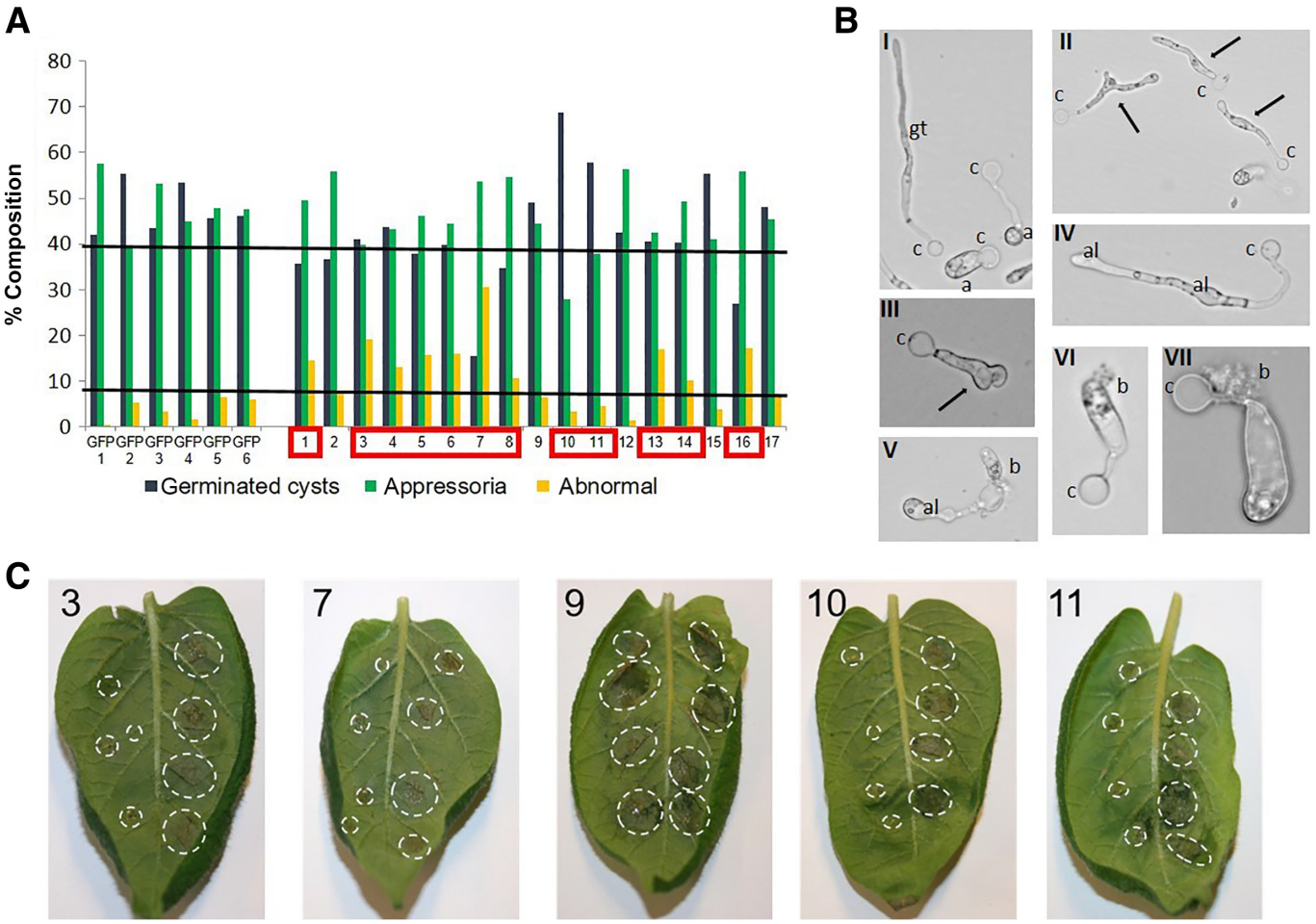

Fig. 8. RNA interference (RNAi)-based transient silencing of elicitor transglutaminases (TGases). **A,** Percentage of germinated cysts, appressoria structures, and abnormal structures counted in individual silenced lines and individual non-endogenous (green fluorescent protein [GFP]) control lines. The lines marked in red were less virulent than the control ones. The horizontal lines are arbitrary thresholds for the minimal number of healthy appressoria structures (upper) and maximum number of abnormal structures (lower) for a line to be pathogenic. **B,** Inverted light microscope images of the counted structures. I: GFP controls with healthy cysts (c), germ tubes (gt), and appressoria (a); II and III: swelling and multiple germ tubes; IV and V: appressorium-like structure (al); V, VI, and VII: bursting (b) of appressoria and cyst. **C,** Detached leaf assay (DLA). Potato leaves were inoculated with four drops of cyst solution from different RNAi lines on the left side and GFP control lines on the right side of the main vein. The RNAi line is indicated in the top left corner of each picture. Pictures were taken 4 days postinoculation. The RNAi experiment was repeated four times with the number of retrieved lines varying from 8 to 18. All the presented results come from the same experiment. As each individual RNAi line is unique and the silencing is transient, phenotyping and genotyping of individual lines could not be repeated.

RNAi-based transient silencing assay. Targeting all genes resulted in almost no recovery, showing that the TGase family of interest is vital for the survival and functioning of *P. infestans*. The efficiency of the RNAi assay was reduced by redesigning the reverse primer to make it less specific. This approach yielded a wide variety of phenotypes ranging from lethal to completely benign. Detailed study of the percentage composition of ungerminated and germinated cysts, appressoria, and any possible abnormalities, combined with pathogenicity assays, allowed us to draw several conclusions.

The observed phenotypes were very similar to the ones observed in cystamine treatments, strengthening the hypothesis that cystamine is indeed an inhibitor of TGase activity. Additionally, what determined pathogenicity of a line was not only the low percentage of abnormal structures formed but the number of healthy appressoria.

Bronkhorst et al. (2021, 2022) investigated the biomechanics of host plant invasion by *P. infestans* and suggested that appressoria or appressoria-like structures are not as important for infection as previously thought. The authors described a slicing mechanism, which they termed "naifu invasion," in which the penetration of host tissue occurs through sharpening of the tip of the germ tube, which then exerts concentrated force at an oblique angle (Bronkhorst et al. 2021). In a follow-up study, the authors elucidated the mechanism by which the hyphal tip can achieve the force required to break through plant tissue. The tip sharpness is controlled by actin rearrangements (Bronkhorst et al. 2022). Even though the two studies describe a mechanism that excludes the need for appressoria formation, we believe there is a possibility that "naifu invasion" and appressoria can coexist. In the naifu mechanism, the hyphal tip exerts force on the plant leaf surface. This initial incision could possibly provide an entry point for an appressorium-like structure that, thanks to its elevated turgor pressure, can push through the cell wall of the plant cell and allow for penetration of the cells. Alternatively, the appressoria structures observed in this study may simply represent swollen hyphal tips that need to build turgor pressure at the tip to exert the force needed to allow the "naifu" knife to penetrate the leaf tissue. Therefore, the appressorium-like structures seen in the current study may simply be penetration structures that are swollen hyphal tips. However, to build the pressure required for slicing and penetration of the plant leaf, septa are likely to be required, because *P. infestans* mycelia are coenocytic. Thus, a new compartment may be formed that superficially resembles an appressorium and acts as a penetration structure to facilitate invasion.

Finally, comparison of the phenotype, pathogenicity, and gene expression data suggests that neither of the investigated TGases was essential for the development of cysts and appressoria on its own, but a certain expression level was necessary, indicating that the proteins are redundant to some extent. Nonetheless, decreased expression of *PITG_16956* in all of the RNAi lines with decreased virulence points toward the role of this particular gene in the development of infection structures necessary for pathogenicity and is consistent with its high expression in germinated cysts.

Acknowledgments

We thank Hadis Mostafanezhad for her help with microscopic observations and Kristian Persson Hodén for his input in the discussion on TGase expression in *P. infestans* oospores.

Literature Cited

Abraham, Y., and Elbaum, R. 2013. Quantification of microfibril angle in secondary cell walls at subcellular resolution by means of polarized light microscopy. New Phytol. 197:1012-1019.

Avrova, A. O., Venter, E., Birch, P. R. J., and Whisson, S. C. 2003. Profiling and quantifying differential gene transcription in *Phytophthora infestans* prior to and during the early stages of potato infection. Fungal Genet. Biol. 40: 4-14.

Beninati, S., Iorio, R. A., Tasco, G., Serafini-Fracassini, D., Casadio, R., and Del Duca, S. 2013. Expression of different forms of transglutaminases by immature cells of *Helianthus tuberosus* sprout apices. Amino Acids 44:271-283.

Bischoff, V., Nita, S., Neumetzler, L., Schindelasch, D., Urbain, A., Eshed, R., Persson, S., Delmer, D., and Scheible, W.-R. 2010. *TRICHOME BIREFRINGENCE* and its homolog *AT5G01360* encode plant-specific DUF231 proteins required for cellulose biosynthesis in Arabidopsis. Plant Physiol. 153:590-602.

Brand, A. 2012. Hyphal growth in human fungal pathogens and its role in virulence. Int. J. Microbiol. 2012:517529.

Bronkhorst, J., Kasteel, M., Van Veen, S., Clough, J. M., Kots, K., Buijs, J., Van Der Gucht, J., Ketelaar, T., Govers, F., and Sprakel, J. 2021. A slicing mechanism facilitates host entry by plant-pathogenic *Phytophthora*. Nat. Microbiol. 6:1000-1006.

Bronkhorst, J., Kots, K., De Jong, D., Kasteel, M., Van Boxmeer, T., Joemmanbaks, T., Govers, F., Van Der Gucht, J., Ketelaar, T., and Sprakel, J. 2022. An actin mechanostat ensures hyphal tip sharpness in *Phytophthora infestans* to achieve host penetration. Sci. Adv. 8:eabo0875.

Brunner, F., Rosahl, S., Lee, J., Rudd, J. J., Geiler, C., Kauppinen, S., Rasmussen, G., Scheel, D., and Nürnberger, T. 2002. Pep-13, a plant defense-inducing pathogen-associated pattern from *Phytophthora* transglutaminases. EMBO J. 21:6681-6688.

Caten, C. E., and Jinks, J. L. 1968. Spontaneous variability of single isolates of *Phytophthora infestans*. I. Cultural variation. Can. J. Bot. 46:329-348.

Cranston, E. D., and Gray, D. G. 2008. Birefringence in spin-coated films containing cellulose nanocrystals. Colloids Surf. A: Physicochem. Eng. Asp. 325:44-51.

Eckert, R. L., Kaartinen, M. T., Nurminskaya, M., Belkin, A. M., Colak, G., Johnson, G. V. W., and Mehta, K. 2014. Transglutaminase regulation of cell function. Physiol. Rev. 94:383-417.

Evangelisti, E., and Govers, F. 2024. Roadmap to success: How oomycete plant pathogens invade tissues and deliver effectors. Annu. Rev. Microbiol. 78:493-512.

Fabritius, A. L., and Judelson, H. S. 2003. A mating-induced protein of *Phytophthora infestans* is a member of a family of elicitors with divergent structures and stage-specific patterns of expression. Mol. Plant-Microbe Interact. 16:926-935.

Folk, J. E. 1980. Transglutaminases. Annu. Rev. Biochem. 49:517-531.

Folk, J. E., and Cole, P. W. 1966. Mechanism of action of guinea pig liver transglutaminase. I. Purification and properties of the enzyme: Identification of a functional cysteine essential for activity. J. Biol. Chem. 241:5518-5525.

Giordano, D., and Facchiano, A. 2019. Classification of microbial transglutaminases by evaluation of evolution trees, sequence motifs, secondary structure topology and conservation of potential catalytic residues. Biochem. Biophys. Res. Commun. 509:506-513.

Grenville-Briggs, L. J., Anderson, V. L., Fugelstad, J., Avrova, A. O., Bouzenzana, J., Williams, A., Wawra, S., Whisson, S. C., Birch, P. R. J., Bulone, V., and van West, P. 2008. Cellulose synthesis in *Phytophthora infestans* is required for normal appressorium formation and successful infection of potato. Plant Cell 20:720-738.

Grenville-Briggs, L. J., Avrova, A. O., Hay, R. J., Bruce, C. R., Whisson, S. C., and van West, P. 2010. Identification of appressorial and mycelial cell wall proteins and a survey of the membrane proteome of *Phytophthora infestans*. Fungal Biol. 114:702-723.

Griffin, M., Casadio, R., and Bergamini, C. M. 2002. Transglutaminases: Nature's biological glues. Biochem. J. 368:377-396.

Guo, J., Chen, S., Huang, C., Chen, L., Studholme, D. J., Zhao, S., and Yu, L. 2004. MANSC: A seven-cysteine-containing domain present in animal membrane and extracellular proteins. Trends Biochem. Sci. 29:172-174.

Hahlbrock, K., Scheel, D., Logemann, E., Nürnberger, T., Parniske, M., Reinold, S., Sacks, W. R., and Schmelzer, E. 1995. Oligopeptide elicitor-mediated defense gene activation in cultured parsley cells. Proc. Natl. Acad. Sci. U.S.A. 92:4150-4157.

Howard, R. J., Ferrari, M. A., Roach, D. H., and Money, N. P. 1991. Penetration of hard substrates by a fungus employing enormous turgor pressures. Proc. Natl. Acad. Sci. U.S.A. 88:11281-11284.

Iranzo, M., Aguado, C., Pallotti, C., Cañizares, J. V., and Mormeneo, S. 2002. Transglutaminase activity is involved in *Saccharomyces cerevisiae* wall construction. Microbiology 148:1329-1334.

Jeitner, T. M., Pinto, J. T., and Cooper, A. J. L. 2018. Cystamine and cysteamine as inhibitors of transglutaminase activity *in vivo*. Biosci. Rep. 38:BSR20180691.

Jones, P., Binns, D., Chang, H.-Y., Fraser, M., Li, W., McAnulla, C., McWilliam, H., Maslen, J., Mitchell, A., Nuka, G., Pesseat, S., Quinn, A. F., Sangrador-Vegas, A., Scheremetjew, M., Yong, S.-Y., Lopez, R., and Hunter, S. 2014. InterProScan 5: Genome-scale protein function classification. Bioinformatics 30:1236-1240.

Jumper, J., Evans, R., Pritzel, A., Green, T., Figurnov, M., Ronneberger, O., Tunyasuvunakool, K., Bates, R., Žídek, A., Potapenko, A., Bridgland, A., Meyer, C., Kohl, S. A. A., Ballard, A. J., Cowie, A., Romera-Paredes, B., Nikolov, S., Jain, R., Adler, J., Back, T., Petersen, S., Reiman, D., Clancy, E., Zielinski, M., Steinegger, M., Pacholska, M., Berghammer, T., Bodenstein, S., Silver, D., Vinyals, O., Senior, A. W., Kavukcuoglu, K., Kohli, P., and Hassabis, D. 2021. Highly accurate protein structure prediction with AlphaFold. Nature 596:583-589.

Katoh, K., Hammar, K., Smith, P. J. S., and Oldenbourg, R. 1999. Birefringence imaging directly reveals architectural dynamics of filamentous actin in living growth cones. Mol. Biol. Cell 10:197-210.

Kelley, L. A., Mezulis, S., Yates, C. M., Wass, M. N., and Sternberg, M. J. E. 2015. The Phyre2 web portal for protein modeling, prediction and analysis. Nat. Protoc. 10:845-858.

Kieliszek, M., and Misiewicz, A. 2014. Microbial transglutaminase and its application in the food industry. A review. Folia Microbiol. 59:241-250.

Lorand, L., and Graham, R. M. 2003. Transglutaminases: Crosslinking enzymes with pleiotropic functions. Nat. Rev. Mol. Cell Biol. 4:140-156.

Madeira, F., Park, Y. M., Lee, J., Buso, N., Gur, T., Madhusoodanan, N., Basutkar, P., Tivey, A. R. N., Potter, S. C., Finn, R. D., and Lopez, R. 2019. The EMBL-EBI search and sequence analysis tools APIs in 2019. Nucleic Acids Res. 47:W636-W641.

Makarova, K. S., Aravind, L., and Koonin, E. V. 1999. A superfamily of archaeal, bacterial, and eukaryotic proteins homologous to animal transglutaminases. Protein Sci. 8:1714-1719.

Martins, I. M., Matos, M., Costa, R., Silva, F., Pascoal, A., Estevinho, L. M., and Choupina, A. B. 2014. Transglutaminases: Recent achievements and new sources. Appl. Microbiol. Biotechnol. 98:6957-6964.

Matson, M. E. H., Liang, Q., Lonardi, S., and Judelson, H. S. 2022. Karyotype variation, spontaneous genome rearrangements affecting chemical insensitivity, and expression level polymorphisms in the plant pathogen *Phytophthora infestans* revealed using its first chromosome-scale assembly. PLoS Pathog. 18:e1010869.

Meng, S., Torto-Alalibo, T., Chibucos, M. C., Tyler, B. M., and Dean, R. A. 2009. Common processes in pathogenesis by fungal and oomycete plant pathogens, described with Gene Ontology terms. BMC Microbiol. 9:S7.

Michel, B. E. 1983. Evaluation of the water potentials of solutions of polyethylene glycol 8000 both in the absence and presence of other solutes. Plant Physiol. 72:66-70.

Money, N. P. 1990. Measurement of hyphal turgor. Exp. Mycol. 14:416-425.

Niu, X., Ah-Fong, A. M. V., Lopez, L. A., and Judelson, H. S. 2018. Transcriptomic and proteomic analysis reveals wall-associated and glucan-degrading proteins with potential roles in *Phytophthora infestans* sexual spore development. PLoS One 13:e0198186.

Nürnberger, T., Nennstiel, D., Jabs, T., Sacks, W. R., Hahlbrock, K., and Scheel, D. 1994. High affinity binding of a fungal oligopeptide elicitor to parsley plasma membranes triggers multiple defense responses. Cell 78:449-460.

Parrotta, L., Tanwar, U. K., Aloisi, I., Sobieszczuk-Nowicka, E., Arasimowicz-Jelonek, M., and Del Duca, S. 2022. Plant transglutaminases: New insights in biochemistry, genetics, and physiology. Cells 11:1529.

Reiss, K., Kirchner, E., Gijzen, M., Zocher, G., Löffelhardt, B., Nürnberger, T., Stehle, T., and Brunner, F. 2011. Structural and phylogenetic analyses of the GP_{42} transglutaminase from *Phytophthora sojae* reveal an evolutionary relationship between oomycetes and marine *Vibrio* bacteria. J. Biol. Chem. 286:42585-42593.

Resjö, S., Brus, M., Ali, A., Meijer, H. J. G., Sandin, M., Govers, F., Levander, F., Grenville-Briggs, L., and Andreasson, E. 2017. Proteomic analysis of *Phytophthora infestans* reveals the importance of cell wall proteins in pathogenicity. Mol. Cell. Proteomics 16:1958-1971.

Reyna-Beltrán, E., Isaac Bazán Méndez, C., Iranzo, M., Mormeneo, S., and Pedro Luna-Arias, J. 2019. The cell wall of *Candida albicans*: A proteomics view. In: *Candida albicans*. IntechOpen. http://dx.doi.org/10.5772/intechopen.82348

Ruiz-Herrera, J., Iranzo, M., Elorza, M. V., Sentandreu, R., and Mormeneo, S. 1995. Involvement of transglutaminase in the formation of covalent cross-links in the cell wall of *Candida albicans*. Arch. Microbiol. 164: 186-193.

Sarkar, N. K., Clarke, D. D., and Waelsch, H. 1957. An enzymically catalyzed incorporation of amines into proteins. Biochim. Biophys. Acta 25: 451-452.

Serafini-Fracassini, D., and Del Duca, S. 2008. Transglutaminases: Widespread cross-linking enzymes in plants. Ann. Bot. 102:145-152.

Tamura, K., Stecher, G., and Kumar, S. 2021. MEGA11: Molecular Evolutionary Genetics Analysis Version 11. Mol. Biol. Evol. 38:3022-3027.

Taylor, J. G., Owen, T. P., Jr., Koonce, L. T., and Haigler, C. H. 1992. Dispersed lignin in tracheary elements treated with cellulose synthesis inhibitors provides evidence that molecules of the secondary cell wall mediate wall patterning. Plant J. 2:959-970.

Torres Ascurra, Y. C., Zhang, L., Toghani, A., Hua, C., Rangegowda, N. J., Posbeyikian, A., Pai, H., Lin, X., Wolters, P. J., Wouters, D., De Blok, R., Steigenga, N., Paillart, M. J. M., Visser, R. G. F., Kamoun, S., Nürnberger, T., and Vleeshouwers, V. G. A. A. 2023. Functional diversification of a wild potato immune receptor at its center of origin. Science 381:891-897.

Tzelepis, G., Hodén, K. P., Fogelqvist, J., Åsman, A. K. M., Vetukuri, R. R., and Dixelius, C. 2020. Dominance of mating type A1 and indication of epigenetic effects during early stages of mating in *Phytophthora infestans*. Front. Microbiol. 11:252.

Varadi, M., Anyango, S., Deshpande, M., Nair, S., Natassia, C., Yordanova, G., Yuan, D., Stroe, O., Wood, G., Laydon, A., Žídek, A., Green, T., Tunyasuvunakool, K., Petersen, S., Jumper, J., Clancy, E., Green, R., Vora, A., Lutfi, M., Figurnov, M., Cowie, A., Hobbs, N., Kohli, P., Kleywegt, G., Birney, E., Hassabis, D., and Velankar, S. 2022. AlphaFold protein structure database: Massively expanding the structural coverage of protein-sequence space with high-accuracy models. Nucleic Acids Res. 50:D439-D444.

Wang, Z.-Y., Jenkinson, J. M., Holcombe, L. J., Soanes, D. M., Veneault-Fourrey, C., Bhambra, G. K., and Talbot, N. J. 2005. The molecular biology of appressorium turgor generation by the rice blast fungus *Magnaporthe grisea*. Biochem. Soc. Trans. 33:384-388.

Zahid, M. A., Sandroni, M., Vetukuri, R. R., and Andreasson, E. 2021. A fast, nondestructive method for the detection of disease-related lesions and wounded leaves. Biotechniques 71:425-430.

Zhong, M., Wang, Y., Zhang, Y., Shu, S., Sun, J., and Guo, S. 2019. Overexpression of transglutaminase from cucumber in tobacco increases salt tolerance through regulation of photosynthesis. Int. J. Mol. Sci. 20:894.